The International Journal of Cardiovascular Imaging (2019) 35:761–769
https://doi.org/10.1007/s10554-018-1509-8

ORIGINAL PAPER

Insights into functional mitral regurgitation using the average pixel intensity method

Victor Kamoen[1] · Milad El Haddad[1] · Tine De Backer[1] · Marc De Buyzere[1] · Frank Timmermans[1]

Received: 12 September 2018 / Accepted: 24 November 2018 / Published online: 3 December 2018

Abstract

Previously we introduced and validated the average pixel intensity (API) method for grading mitral regurgitation (MR) in a heterogeneous MR population. We now investigated the feasibility and added value of the API method more specifically in patients with functional MR (FMR). We consecutively enrolled 283 patients with pure FMR. Transthoracic echocardiography was performed and MR was assessed using the API method and guideline-recommended parameters, including color Doppler, vena contracta width (VCW) and proximal isovelocity surface area (PISA)-based methods. The API method had an applicability of 98% in this FMR cohort, which was significantly higher than VCW (84%) and PISA-based methods (75%). Overall, the API method had significant correlations with direct parameters of FMR severity, ejection fraction, atrial and ventricular dimensions, pulmonary pressures and New York Heart Association class. Analysis of the API dynamics during MR revealed a typical pattern with early and late systolic peaks in API and a midsystolic nadir, which matched the temporal changes of the effective regurgitant orifice (ERO) during FMR. Based on ROC curves of established FMR severity cut-offs, an API value of 125 au was considered the optimal cut-off to determine severe MR. Interestingly, this API severity cut-off is similar to the API severity cut-off for MR in degenerative MR (DMR), despite different EROA/RV cut-offs in current ESC guidelines for FMR and DMR. The API method is an easy, fast and feasible parameter for grading FMR and may complement the multiparametric assessment of FMR in daily clinical practice.

Keywords Mitral regurgitation · Echocardiography · Continuous Wave Doppler · Average pixel intensity method

Introduction

Systolic heart failure is frequently complicated by secondary/functional mitral regurgitation (FMR). The presence of FMR is widely recognized as a marker of adverse outcome in ischemic and non-ischemic cardiomyopathy, however, as FMR is mainly a consequence of intrinsic ventricular disease, it is still contested whether FMR is an independent predictor of mortality in heart failure patients [1–3]. Surgical correction of FMR also remains controversial as the benefits on overall prognosis are not clear [4–6]. Since FMR is a disease involving a multitude of interrelated variables, predicting the impact of a given regurgitant load on the already diseased and evolving ventricle remains problematic [1]. Hence, defining "severe" FMR is a complex issue that is further complicated by echocardiographic challenges in grading FMR [7] and the fact that different "severity" cut-offs are proposed by American [Effective regurgitant orifice area (EROA) and regurgitant volume (RV): 0.4 cm^2 and 60 ml, respectively] versus European heart associations (EROA and RV: 0.2 cm^2 and 30 ml, respectively). These guidelines emphasize the importance of a multiparametric approach for grading MR severity, including qualitative (e.g. color Doppler), semi-quantitative [vena contracta width (VCW)] and quantitative (e.g. EROA and RV) parameters [7–10]. Importantly, the feasibility to assess EROA in FMR has been highly variable, ranging from 8 to 81% [1]. Moreover, a flattened hemispheric flow convergence zone is frequently found in FMR, which may lead to underestimated proximal isovelocity surface area (PISA)-EROA and PISA-RV values [1, 7]. Finally, all outcome studies in FMR on which

Electronic supplementary material The online version of this article (https://doi.org/10.1007/s10554-018-1509-8) contains supplementary material, which is available to authorized users.

✉ Victor Kamoen
victor.kamoen@ugent.be

[1] Department of Cardiology, Heart Center, Ghent University Hospital, Cornelis Heymanslaan 10, 10-K12, 9000 Ghent, Belgium

guidelines are based, have combined different methods and averaged EROA/RV values, which is rarely performed in daily clinical practice [11, 12].

We previously introduced the average pixel intensity (API) method for grading MR severity based on the intensity measure of the continuous wave (CW) Doppler signal of the MR flow [13]. This method integrates the time-varying flow during mitral regurgitation (MR) in a single measure and avoids geometric assumptions such as encountered in PISA, VCW and Doppler methods. We also showed that this API method has a higher applicability rate and better inter- and intraobserver agreement than guideline-recommended measures. We now aim to assess the API method in patients with pure FMR and position the API method within this multi-integrative FMR approach. More specifically, we focused on feasibility, flow dynamics and hydraulics in FMR and we determined API severity cut-offs for FMR.

Materials and methods

Patient selection and transthoracic echocardiography

We prospectively enrolled 288 patients at the department of cardiology of the University Hospital Gent between 2014 and 2017. All echocardiographic examinations were performed on VIVID E9 XDclear echo machine (General Electric, Horten, Norway; M5Sc-D probe). Only patients with pure FMR, i.e. absence of a degenerative mitral valve apparatus causing (part of the) MR, were considered after careful analysis of all recordings and independent of ejection fraction (EF). Patients were dichotomized to ejection fraction (EF) < 40% and EF > 40% [14]. The study was approved by the local Ethics Committee.

Echocardiographic assessment of MR

All echocardiographic acquisitions were performed by a single and experienced operator (FT). The API method was applied as previously reported [13]. In brief, the API is calculated using an offline custom-made program which converts uncompressed red–green–blue (RGB) DICOM files exported from the echo machine into grayscale images (range 0–255 arbitrary units). The operator (VK), blinded to the clinical and echocardiographic characteristics of the patients, then selects the area of interest within the CW envelope (i.e. starting from mitral closure or beginning of the CW envelope) and the program automatically calculates the average of the pixels intensity (API) of the selected area. The Doppler gain level was fixed at 6 dB for all patients to reduce undersaturation of the signal in the mildest MR and oversaturation in the most severe MR (i.e. intensity of almost all pixels was > 0 and < 255 au). Patients with ≥ 2 large MR jets were excluded from analysis. To study API dynamics during MR, the systolic cycle was automatically divided into three phases with equal duration: a proto-(T1), mid-(T2) and telesystolic (T3) phase and the API values were calculated for each phase.

The vena contracta width (VCW) was assessed as previously reported [13]. EROA and RV were calculated using proximal isovelocity surface area (PISA) method according to consensus recommendations [7, 9]. For acquisition of the PISA radii, the aliasing velocity was set at 25 cm/s. Patients without a proper or reproducible flow convergence zone (FCZ), e.g. because of extreme flattening of the FCZ or suboptimal VCW were excluded from analysis. Color Doppler grading of the MR jet (1–4) was performed using parasternal long axis (PSLAX), apical two (AP2CH), four (AP4CH) and five chamber (AP5CH) views, as previously described [7, 15]. The annular diameter was measured in PSLAX during systole and diastole [9].

Statistical analysis

Continuous variables were expressed as mean ± standard deviation (SD) (or median with interquartile range (IQR) for non-normal distributions) and dichotomous variables as percentage. Normality of data distribution was tested with Shapiro–Wilk test. Analysis of variance (ANOVA) test or Kruskal–Wallis test (for continuous variables) and χ^2 test (for dichotomous variables) were used to evaluate significant group differences. Linear trend among quartiles was evaluated with Jonckheere–Terpstra test or Mantel linear-by-linear test. Correlations were calculated using Pearson's coefficient and Spearman's rank order coefficient. All statistical analyses were performed in SPSS Statistics V.24 (IBM, Armonk, New York, USA). Receiver operating characteristic (ROC) curves were created using SigmaPlot (Systat, San Jose, USA). p Values < 0.05 were considered statistically significant. Multivariate analysis models are described where appropriately.

Results

Feasibility

The API method was applicable in 283 out of 288 patients (98%). Reasons for non-applicability were the presence of large multiple (≥ 2) MR jets in 5 patients. Quantification of MR by PISA-based methods and VCW was feasible in 75% and 84% of all FMR patients, respectively, which was significantly lower than the API applicability (p < 0.001).

Clinical and echocardiographic parameters

Table 1 shows the clinical and echocardiographic characteristics of the FMR cohort, according to API quartiles (Q1–Q4) and EF < 40% or > 40%. Along with increasing API values, there is a steady increase of other direct parameters of FMR severity, including PISA-EROA, PISA-RV, VCW and color Doppler grade (all p for trend < 0.001). API has statistical significant correlations with these indices (Supplemental Table 1), as well as with the functional and structural cardiac parameters, such as ventricular and atrial dimensions and pulmonary pressures (Table 1). In contrast to patients with EF > 40%, in the subgroup of patients with reduced EF (EF < 40%) a significant association between API and tenting area was observed (p 0.039). Also, the EF does not alter significantly along the increasing quartiles in EF > 40%, and this population has less severe MR. In fact, Table 1 shows that patients with EF > 40% have less mitral tenting, more frequently atrial fibrillation (AF), less ventricular dilation and smaller left atrial (LA) dimensions

Table 1 Clinical and echocardiographic characteristics according to API quartiles

	EF < 40%					EF > 40%				
	Q1	Q2	Q3	Q4	p	Q1	Q2	Q3	Q4	p
n	35	32	36	32		35	38	37	35	
BMI (kg/m^2)	25.9	27.1	26	25.6	0.448*	27.1	25.7	27.4	24.8	**0.047***
BSA (m^2)	1.89	1.9	1.87	1.88	0.914*	1.84	2.46	1.91	1.79	0.395*
RR (ms)	877	813	808	767	0.132*	921	1009	961	854	**0.031***
LVEDD/BSA (mm/m^2)	30	31	33	35	**0.001**†	26	26	28	29	0.774†
LVESD/BSA (mm/m^2)	24	25	29	32	**0.001***	19.5	19	20	22.3	**0.006***
LA vol/BSA (ml/m^2)	42	48	63	56	**0.001** †	41	48	49	56	0.259†
LV mass/BSA (g/m^2)	130	122	146	157	**0.024**†	103	114	118	120	0.795†
EDV/BSA (ml/m^2)	78	80	90	101	**0.002**†	52	51	54	65	0.85†
ESV/BSA (ml/m^2)	51	54	61	73	**0.001**†	23	22	27	33	0.393†
Ann diameter (cm) D	3.8	3.9	4.1	4.3	**0.006***	3.7	3.8	4.1	4	**0.041***
Ann diameter (cm) S	3.3	3.3	3.7	3.7	**0.004***	3.2	3.3	3.5	3.6	0.064*
Ads/Add	0.85	0.86	0.9	0.88	0.284†	0.85	0.87	0.86	0.9	0.426†
EF (%)	33	32	30	29	**0.028***	55	55	53	50	0.068*
NYHA class	1.45	1.93	1.94	2.44	**0.001**†	1.32	1.36	1.52	2.07	**0.001**†
RVSP (mmHg)	40	40	48	50	**0.01**†	36	42	38	45	**0.027**†
MRd (ms)	469	460	431	429	**0.031**†	443	467	462	438	0.122†
Avg API	70	107	135	173	**0.001***	58	87	114	147	**0.001***
Color Doppler grade	2	2	3	3	**0.001**†	1	2	3	3	**0.001**†
VCW (mm)	4	4.6	6.2	6.4	**0.001**†	3.7	4.1	4.8	5.9	**0.001**†
PISA radius (mm)	5.5	6.5	8.4	8.8	**0.001***	5.1	6.4	6.6	7.6	**0.013***
PISA EROA (cm^2)	0.12	0.14	0.22	0.25	**0.001**†	0.07	0.12	0.14	0.15	**0.01**†
PISA RV (ml)	16	24	36	39	**0.001**†	15	21	24	28	**0.01**†
Vmax (cm/s)	496	507	490	478	0.418*	539	553	568	558	0.253*
Vmean (cm/s)	364	378	364	347	0.152*	406	424	430	420	0.21*
Vmax/Vmean	1.36	1.34	1.37	1.37	0.384†	1.31	1.3	1.32	1.34	0.501†
TVI (cm)	165	177	162	160	0.475*	179	196	199	191	0.292*
Tenting height (cm)	0.7	0.7	0.7	0.9	0.053*	0.6	0.7	0.6	0.6	0.739*
Tenting area (cm^2)	1.2	1.6	1.5	1.9	**0.039***	1.1	1.2	1.1	1.1	0.8*

The p-values in bold indicate statistical significance

BMI body mass index, *BSA* body surface area, *SBP* systolic blood pressure, *DBP* diastolic blood pressure, *RR* R-to-R interval, *AF* atrial fibrillation, *LV* left ventricle, *LVEDD* LV end diastolic diameter, *LVESD* LV end systolic diameter, *LVEDV* LV end diastolic volume, *LVESV* LV end systolic volume, *LA* left atrium, *MRd* mitral regurgitation duration, *EF* ejection fraction, *RVSP* right ventricle systolic pressure, *VCW* vena contracta width, *PISA* proximal isovelocity surface area, *PISA-EROA* PISA effective regurgitant orifice area, *PISA-RV* PISA regurgitant volume, *MR* mitral regurgitation, *TVI* time-velocity integral, *ADd* annular diameter in diastole, *ADs* annular diameter in systole, *NYHA* New York Heart Association

*Analysis of Variance (ANOVA) test

†Kruskal–Wallis test

(all $p < 0.005$), pointing to a different population compared to EF < 40%.

Dynamic changes in pixel intensity

The FMR CW envelopes were divided into three equal phases (proto-(T1), mid-(T2) and telesystolic (T3)) (Fig. 1, panel a) and for each phase, API, PISA-EROA and PISA-RV are calculated. Figure 1, panel b shows a representative example of a triphasic API pattern, elevated in T1 and T3 and with a midsystolic API nadir in T2 phase. Below, the average T1–T2–T3 dynamics are tabulated for API (n = 283) and for PISA-EROA/PISA-RV (n = 38). This triphasic pattern remained consistent in all subgroups and was independent of heart rhythm, tenting height/area, annular diameter or EF in multivariable analysis (data not shown). For PISA-EROA we observed a similar pattern with the highest values in early and late systole and a midsystolic decrease in T2. For the RV, T1 and T3 values were somewhat lower than the midsystolic RV.

To further illustrate how a fluctuating MR flow can be easily captured by the API method, we investigated MR severity and T1–T2–T3 dynamics in 11 FMR patients with frequent monomorphic ventricular extrasystoles (VES) (non-bigeminy) during echo examination and calculated the API during the VES-MR (Supplemental Fig. 2). The CW envelopes of the VES-MR had the same triphasic pattern as described above. Interestingly, the VES itself resulted in significantly higher API values (and thus more FMR) compared to the pre- and post VES.

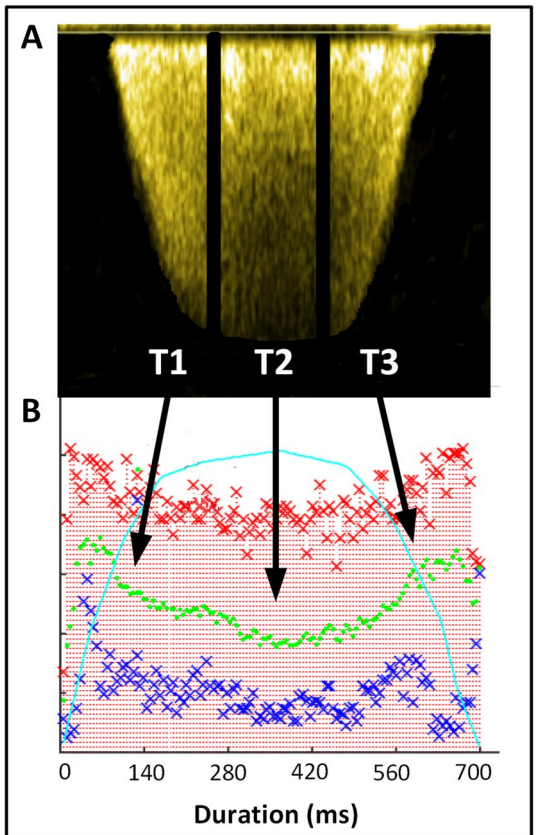

N = 283	T1	T2	T3	p
API (au)	126	101	108	<0.001
PISA-EROA (cm²)	0.23	0.19	0.3	<0.001
PISA-RV (ml)	11.1	15	13.8	<0.001

Fig. 1 Analysis of API kinetics during FMR. The CW envelope is traced and divided into three equal time phases (T1, T2 and T3). A representative example is shown. The middle panel graphically depicts the dynamic course of pixel intensities during the systolic cycle (the green line indicates the average pixel intensity). The variation of API, PISA-EROA and PISA-RV is also tabulated below

Relationship between API, TVI, EROA and RV

Panel A and B in Fig. 2 show the relationship of API and PISA-EROA with time-velocity integral (TVI). With increasing MR severity (expressed as API and PISA-EROA), TVI decreases in the overall FMR cohort. However, statistical analysis revealed that in patients with EF > 40% (black dots) (and thus generally lower PISA-EROA values), PISA-EROA did not correlate with TVI ($p = 0.111$), whereas in patients with EF < 40% (bearing higher PISA-EROA values) there is a significant correlation between PISA-EROA and TVI ($p < 0.001$). Figure 2, panel C clearly illustrates the linear relationship between TVI and EF in < 40% EF subjects. As a consequence, in FMR patients with EF > 40%, TVI does not significantly change with increasing PISA-EROA and thus a linear relationship between PISA-EROA and PISA-RV can be expected when considering the hydraulic equation PISA-RV = PISA − EROA × TVI [16]. This contrasts with the EF < 40%, where PISA-EROA and TVI interact inversely and therefore PISA-EROA and PISA-RV are not linearly related. The implication of this differential interaction is depicted in panel D, where the blue line connects the corresponding guideline-recommended EROA and RV cut-off pairs (EROA and RV: 0.2 cm^2–30 ml and 0.4 cm^2–60 ml). Of interest, in the lower EROA ranges, the dots locate to the left side of this line, indicating a relative higher RV for a given EROA, whereas in the higher EROA values (EF < 40%), there is a shift towards the right side of the blue line. This right-sided shift obviously reflects the gradual decrease of TVI with increasing EROA in lower EF ranges. According to this non-linear relationship, the severity cut-off of 0.2 cm^2 (EROA) corresponds to an RV cut-off which is likely to be higher than 30 ml, whereas the 0.4 cm^2 cut-off (AHA/ACC guidelines 2017) most likely corresponds to values lower than the commonly recommended severity cut-off

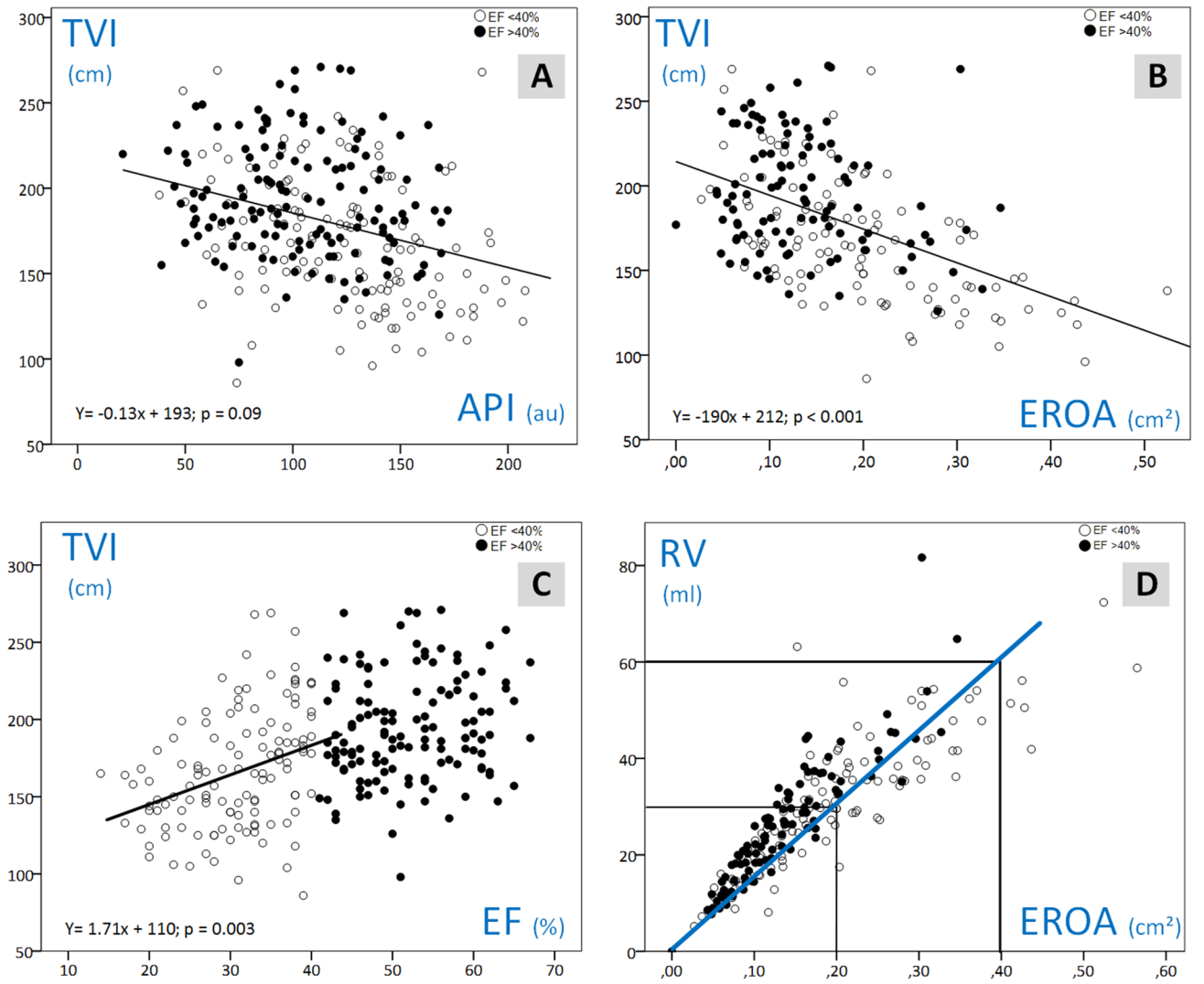

Fig. 2 Interaction of API, PISA-EROA, TVI and EF. **a, b** Depicts the relationship between API/PISA-EROA and TVI. With increasing MR severity, TVI decreases. **c** The relationship between EF and TVI: in patients with EF > 40% (black dots) there is no statistical correlation between EF and TVI, whereas in patients with EF < 40% (white dots) EF and TVI correlate significantly (the regression coefficients apply to patients with EF < 40%). **d** The implication of this differential interaction observed in panel **c**. The blue line connects the recommended cut-off pairs for EROA and RV (0.20 cm^2–30 ml and 0.40 cm^2–60 ml). In the EF > 40% ranges, the black dots locate all on the left side of the blue line, indicating that RV is relatively larger than EROA values. With increasing EROA (and decreasing EF), there is a shift to the right side, which reflects the decreasing TVI values

of 60 ml in FMR. The API method correlates well with TVI, PISA-EROA and PISA-RV but is not hampered by these hydraulic interactions as it does not require any complex calculation with other echocardiographic variables. Finally, we performed multivariate analysis (model including important hydraulic components: TVI, PISA-EROA, EF and RVSP) and this analysis showed that the independent predictors of TVI in EF < 40% are PISA-EROA and EF, whereas in EF > 40%, EF and right ventricular systolic pressure (RVSP) are independently associated with TVI.

Defining API severity cut-offs in FMR

Guidelines have proposed severity cut-offs for FMR based on different MR grading methods [8, 10]. We constructed ROC-curves based on these cut-offs to define the severity cut-off for API in FMR (Fig. 3). For the PISA-based methods we applied the current ESC cut-offs (EROA 0.2 cm^2 and RV 30 ml). Color Doppler grade ≥ 3 corresponded to API 120; PISA-EROA > 0.2 cm^2 corresponded to API 126; PISA-RV > 30 ml corresponded to API 125; VCW > 7 mm [7, 8] corresponded to API 130 (VCW > 4 mm [1] corresponded to

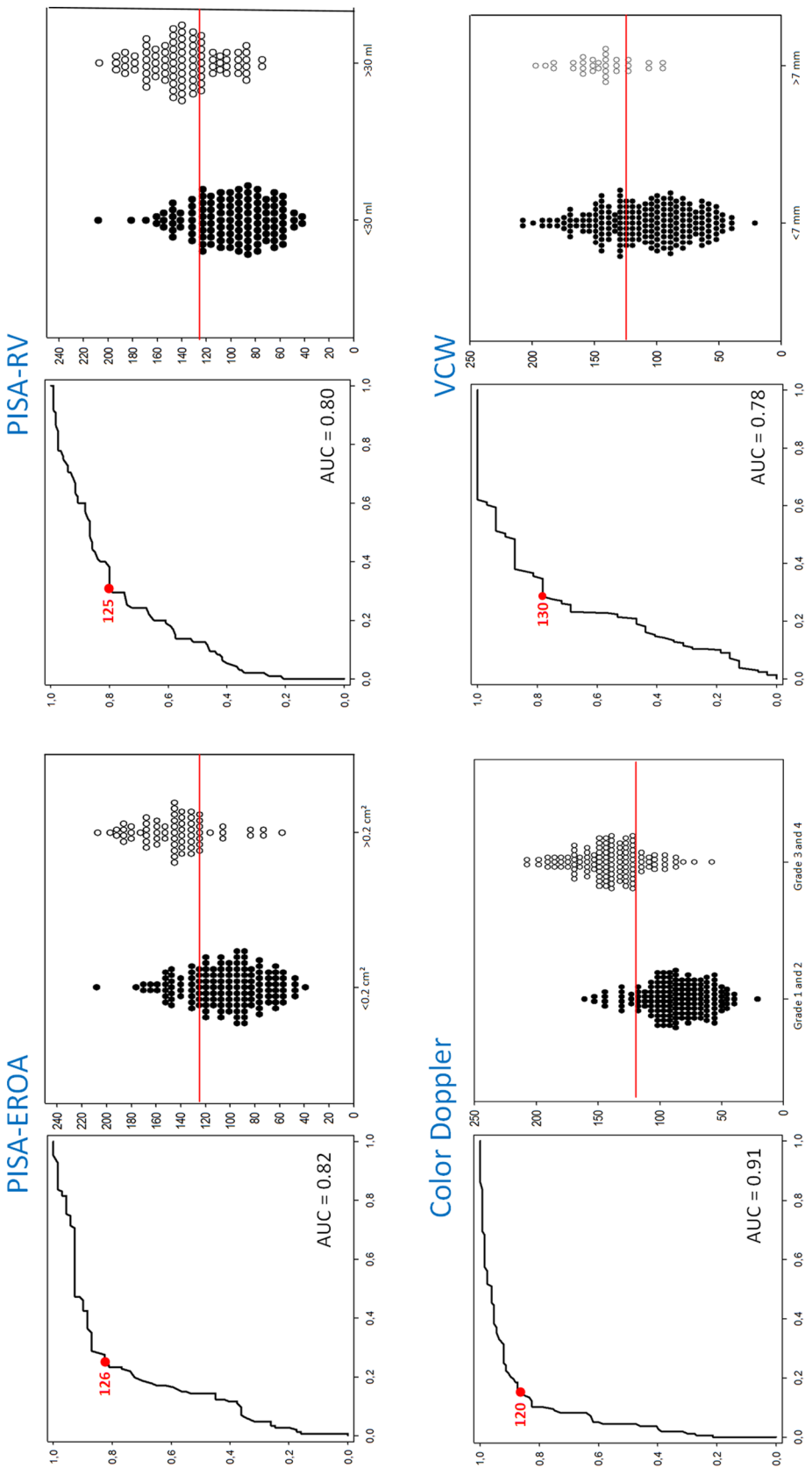

Fig. 3 ROC-curves. ROC curves were constructed on guideline-recommended cut-offs of PISA-EROA, PISA-RV, Color Doppler and VCW to determine a severity cut-off for API in FMR

API 111). Considering the results from the different ROC-curves, we empirically determined an API cut-off of 125 au to identify severe FMR. Of note, we could not determine API cut-offs based on the recently upgraded AHA guidelines for FMR, as there were only 7 patients (3%) with PISA-EROA > 0.4 cm^2 in our cohort.

Guidelines mention the presence of a triangular CW envelope as a sign of severe MR [7, 9]. However, a triangular CW envelope was a rare finding in our chronic FMR population, indicating low sensitivity, but it had a good specificity for severe FMR (based on the API cutoff of 125 au).

Discussion

In the present study, we showed that the API method is a simple and easy approach for grading FMR severity with a feasibility that is higher than conventional methods such as VCW and PISA method. As the API method integrates the time-varying flow during regurgitation (in contrast to PISA and VCW), it avoids geometric assumptions or complex calculations, providing a clear advantage for grading FMR in daily clinical practice.

Determinants of FMR severity

In contrast to primary MR, secondary FMR is caused by LV disease. Assessing the impact of a given regurgitant load on an already diseased ventricle is a very challenging issue, even though we showed significant associations between API and atrial volume, ventricular dimensions, EF and RVSP. Indeed, intervention studies in FMR have shown reduced ventricular dimensions following MV intervention [17, 18], probably due to reverse remodeling and/or volume unloading, indicating that the FMR itself contributes to further LV dilation and/or dysfunction. However, its independent impact on mortality remains disputed [2, 3].

To assess the determinants of "FMR severity", we performed multivariate analysis including the major actors that comprise the Torricelli principle, i.e. RV = ROA (regurgitant orifice area) × Cd × MPG × time (where $\sqrt{\text{MPG} \times \text{time}} = \text{TVI}$ and ROA × Cd = EROA). The mean pressure gradient (MPG) is determined by a complex interplay between afterload, contractility, function and the left atrial pressure [19]. An important observation is that the relation between EROA and RV is not a static, linear correlation, as TVI decreases with increasing EROA in patients with FMR and EF < 40%. Indeed, multivariate analysis identified the independent variables of TVI in EF < 40% being the EROA and EF, whereas in EF > 40%, EF and RVSP are independently associated with TVI, not EROA. The RV/EROA relationship in FMR and DMR has been previously studied by Chiampan et al. [20] and showed that the RV/EROA ratio is lower in FMR compared to degenerative MR (DMR). However, the differential RV/EROA is determined by the TVI behavior, which decreases with increasing EROA and decreasing EF. Consequently, as illustrated in Fig. 2d, an EROA of 0.20 cm^2 corresponds to RV of > 30 ml in FMR, and an EROA of 0.40 cm^2 corresponds to RV values < 60 ml. Thus, it is important to recognize that the "paired" ESC or AHA cut-offs (0.20 cm^2 and 30 ml; 0.40 cm^2 and 60 ml) are not based on hydraulic laws, but both EROA and RV cut-offs have been determined separately based on outcome studies [12]. Anyway, the API method does not suffer from these complex dynamic interactions as it does not require any assumption, calculation or correction with other (echocardiographic) variables because it integrates the complex hemodynamic interactions in a single measure.

Interestingly, a triangular shape of the CW envelope is associated with lower TVI values, but a triangular shape was a rare finding in severe FMR (low sensitivity for severe FMR) but has a good specificity for severe FMR (not shown).

Finally, we found that AF is associated with a reduced systolic annular contraction, probably causing a higher API (and thus FMR) in patients with EF > 40% and may include patients with the so called 'atrial FMR'[21]. In contrast, in patients with EF < 40%, the increasing tenting area and lowered ventricular contractility become the predominant mechanisms of FMR in both sinus rhythm and AF.

Flow dynamics in FMR

Dynamic changes of EROA during FMR have been described previously [22–24] and the API method readily revealed a similar triphasic pattern, with an early- and late-systolic peak and a mid-systolic decline of API. A similar dynamic pattern was seen for EROA, which corroborates the data of Hung et al. [22], but contrasts with the API or MR flow dynamics in holosystolic mitral valve prolapse (MVP) MR, where similar API values are observed in proto, mid and telesystole [15]. In FMR, the RV peaked at mid-systole compared to early and late systole, which may seem paradoxical when considering the EROA and API kinetics. One of the reasons for this observation could relate to the tracing of the entire mid-systolic TVI to calculate RV, despite (very) low pixel intensities at this T2 phase in a considerable amount of subjects, hence overestimating TVI, and thus RV. Indeed, a similar remark holds true for MR in MVP, where TVI tracings are proposed to be restricted to the densest part of the CW envelope area [7, 25]. In addition, the mid-systolic RV may be overestimated due to the artificial division of the MR envelope into three equal phases and this may not match the temporal kinetics of EROA during T2. These observations again illustrate the advantage of the API method where

the tracing of the entire systolic cycle is performed and thus avoiding bias with respect to variable flow dynamics (i.e. pixel intensity) during MR. Finally, our data show an increase in FMR during VES, with normalization of API in the post-extrasystolic beat. Probably, the closing forces in these diseased ventricles further decrease during VES and may improve again following the compensatory pause.

Severity cut-offs in FMR

International guidelines recommend to quantify MR severity by assessing the EROA and RV, however with different severity cut-offs with regard to DMR (EROA: 0.4 cm^2; RV: 60 ml) and FMR (EROA: 0.2 cm^2; RV: 30 ml) [8, 10]. In the present study, we obtained an API severity cut-off of 125 au for FMR, which is similar to the API severity cut-off in DMR [15], despite different EROA/RV cut-offs. This probably indicates that the API method unmasks the underestimation of PISA-based FMR severity, which is supported by the relative higher API value of 75 au/0.1 cm^2 EROA in FMR compared to the API value of 40 au/0.1 cm^2 EROA in DMR [15]. Previous studies have indeed shown that the PISA-method underestimates EROA in FMR [1, 23, 26, 27]. Hence, our data are in agreement with the actual ESC cut-offs and this finding suggests that the API method is likely to be less dependent on the geometry or shape of vena contracta area compared to the PISA-method. Nevertheless, future outcome studies should provide a more solid base for determining API severity cut-off values.

In contrast to the updated ESC guidelines [8], the EROA/RV cut-offs have been upgraded by recent AHA/ACC guidelines [10], with the recommended severity cut-offs for FMR being now the same as for DMR (EROA $\geq$ 0.4 cm^2 and RV $\geq$ 60 ml). This was proposed because even mild degrees of MR may be clinically significant [12] and to avoid unnecessary intervention and procedure-related complications because recent studies have shown that surgical intervention in patients with EROA 0.2–0.4 cm^2 does not improve clinical outcome [7]. However, when reviewing the literature on grading FMR, patients with EROA > 0.4 cm^2 or RV > 60 ml are very rare [1, 28] and represent only 3% of our FMR cohort. Also, in almost all (outcome) studies on FMR (including the recent randomized intervention trials [11, 29]) on which guidelines are based, a combination of methods were used to obtain averaged RV and EROA values [4, 12]. It also remains uncertain how the different methods perform individually, as no head-to-head comparisons are provided in the reports. Finally, this combined approach is rarely performed by cardiologists and therefore the API method may be of added value in daily clinical practice, as it provides a single and fast measure for grading FMR.

Limitations

The limitations of the API method have been discussed previously [13]. In FMR, due to the elliptical or crescentic shape of the ROA, the interrogating area of the CW (which is estimated at 54 mm^2 in our system) may not entirely capture the ROA, thus possibly underestimating true MR severity. We believe that this may be the case in very large elliptical ROA's, but in these subjects, very high API values are obtained already and thus a full coverage of the ROA may not have further clinical implications. Although no gold standard methods exist for grading MR, we did not compare the API method in FMR with other reference methods such as magnetic resonance. Outcome studies are being completed at our center to better define the optimal API cut-offs in FMR.

Compliance with Ethical Standards

Conflict of interest The authors declare that they have no conflict of interest.

References

1. Grayburn PA, Carabello B, Hung J et al (2014) Defining "severe" secondary mitral regurgitation. J Am Coll Cardiol 64:2792–2801
2. Sannino A, Smith RL, Schiattarella GG et al (2017) Survival and cardiovascular outcomes of patients with secondary mitral regurgitation: a systematic review and meta-analysis. JAMA Cardiol 2:1130–1139
3. Mowakeaa S, Dwivedi A, Grossman JR et al (2018) Prognosis of patients with secondary mitral regurgitation and reduced ejection fraction. Open Heart 5:e000745
4. Michler RE, Smith PK, Parides MK et al (2016) Two-year outcomes of surgical treatment of moderate ischemic mitral regurgitation. N Engl J Med 374:1932–1941
5. Wu AH, Aaronson KD, Bolling SF et al (2005) Impact of mitral valve annuloplasty on mortality risk in patients with mitral regurgitation and left ventricular systolic dysfunction. J Am Coll Cardiol 45:381–387
6. Mihaljevic T, Lam B-K, Rajeswaran J et al (2007) Impact of mitral valve annuloplasty combined with revascularization in patients with functional ischemic mitral regurgitation. J Am Coll Cardiol 49:2191–2201
7. Zoghbi WA, Adams D, Bonow RO et al (2017) Recommendations for noninvasive evaluation of native valvular regurgitation. J Am Soc Echocardiogr 30:303–371
8. Baumgartner H, Falk V, Bax JJ et al (2017) 2017 ESC/EACTS guidelines for the management of valvular heart disease. Eur Heart J 38:2739–2791
9. Lancellotti P, Moura L, Pierard LA et al (2010) European Association of echocardiography recommendations for the assessment of valvular regurgitation. Part 2: mitral and tricuspid regurgitation (native valve disease). Eur J Echocardiogr 11:307–332
10. Nishimura RA, Otto CM, Bonow RO et al (2017) 2017 AHA/ACC focused update of the 2014 AHA/ACC Guideline for the management of patients with valvular heart disease. J Am Coll Cardiol 70:252–289

11. Acker MA, Parides MK, Perrault LP et al (2014) Mitral-valve repair versus replacement for severe ischemic mitral regurgitation. N Engl J Med 370:23–32
12. Grigioni F, Enriquez-Sarano M, Zehr KJ et al (2001) Ischemic mitral regurgitation: long-term outcome and prognostic implications with quantitative Doppler assessment. Circulation 103:1759–1764
13. El Haddad M, De Backer T, De Buyzere M et al (2017) Grading of mitral regurgitation based on intensity analysis of the continuous wave Doppler signal. Heart 103:190–197
14. Ponikowski P, Voors AA, Anker SD et al (2016) 2016 ESC Guidelines for the diagnosis and treatment of acute and chronic heart failure. Eur Heart J 37:2129–2200
15. Kamoen V, El Haddad M, De Buyzere M et al (2018) Grading of mitral regurgitation in mitral valve prolapse using the average pixel intensity method. Int J Cardiol 258:305–312
16. Grayburn PA (2011) The importance of regurgitant orifice shape in mitral regurgitation. JACC Cardiovasc Imaging 4:1097–1099
17. Fattouch K, Guccione F, Sampognaro R et al (2009) POINT: efficacy of adding mitral valve restrictive annuloplasty to coronary artery bypass grafting in patients with moderate ischemic mitral valve regurgitation: a randomized trial. J Thorac Cardiovasc Surg 138:278–285
18. Chan KMJ, Punjabi PP, Flather M et al (2012) Coronary artery bypass surgery with or without mitral valve annuloplasty in moderate functional ischemic mitral regurgitation: final results of the randomized ischemic mitral evaluation (RIME) trial. Circulation 126:2502–2510
19. Grayburn PA, Weissman NJ, Zamorano JL (2012) Quantitation of mitral regurgitation. Circulation 126:2005–2017
20. Chiampan A, Nahum J, Leye M et al (2012) Determinants of regurgitant volume in mitral regurgitation: contrasting effect of similar effective regurgitant orifice area in functional and organic mitral regurgitation. Eur Hear J Cardiovasc Imaging 13:324–329
21. Liang JJ, Silvestry FE (2016) Mechanistic insights into mitral regurgitation due to atrial fibrillation: "atrial functional mitral regurgitation". Trends Cardiovasc Med 26:681–689
22. Hung J, Otsuji Y, Handschumacher MD et al (1999) Mechanism of dynamic regurgitant orifice area variation in functional mitral regurgitation: physiologic insights from the proximal flow convergence technique. J Am Coll Cardiol 33:538–545
23. Buck T, Plicht B, Kahlert P et al (2008) Effect of dynamic flow rate and orifice area on mitral regurgitant stroke volume quantification using the proximal isovelocity surface area method. J Am Coll Cardiol 52:767–778
24. Schwammenthal E, Chen C, Benning F et al (1994) Dynamics of mitral regurgitant flow and orifice area. Physiologic application of the proximal flow convergence method: clinical data and experimental testing. Circulation 90:307–322
25. Topilsky Y, Michelena H, Bichara V et al (2012) Mitral valve prolapse with mid-late systolic mitral regurgitation: pitfalls of evaluation and clinical outcome compared with holosystolic regurgitation. Circulation 125:1643–1651
26. Kahlert P, Plicht B, Schenk IM et al (2008) Direct assessment of size and shape of noncircular vena contracta area in functional versus organic mitral regurgitation using real-time three-dimensional echocardiography. J Am Soc Echocardiogr 21:912–921
27. Choi J, Heo R, Hong G-R et al (2014) Differential effect of 3-dimensional color Doppler echocardiography for the quantification of mitral regurgitation according to the severity and characteristics. Circ Cardiovasc Imaging 7:535–544
28. Gaasch WH, Meyer TE (2017) Secondary mitral regurgitation (part 1): volumetric quantification and analysis. Heart heartjnl-2017-312001
29. Smith PK, Puskas JD, Ascheim DD et al (2014) Surgical treatment of moderate ischemic mitral regurgitation. N Engl J Med 371:2178–2188